

<sup>1</sup>Mustefa JIBRIL, <sup>2</sup>Tesfabirhan SHOGA

# $H_{\infty}$ AND $\mu$ - SYNTHESIS DESIGN OF QUARTER CAR ACTIVE SUSPENSION SYSTEM

<sup>1</sup>Department of Electrical & Computer Engineering, DireDawa Institute of Technology, DireDawa, ETHIOPIA

<sup>2</sup>Department of Electrical & Computer Engineering, Jimma Institute of Technology, Jimma, ETHIOPIA

**Abstract:** To improve the road handling and passenger comfort of a vehicle, a suspension system is provided. An active suspension system is considered to be better than the passive suspension system. In this paper, 2 degrees of freedom of a linear quarter car active suspension system is designed, which is subject to different disturbances on the road. Since the parametric uncertainty in the spring, the shock absorber, mass and the actuator has been considered, robust control is used. In this paper,  $H_{\infty}$  and  $\mu$ - synthesis controllers are used to improve the driving comfort and the ability to drive the car on the road. For the analysis of the time domain, using a MATLAB script program and performed a test using four disturbance inputs of the road (bump, random, sinusoidal and harmonic) for the suspension deflection, the acceleration of the body and the body travel for the active suspension with the  $H_{\infty}$  controller and active suspension with  $\mu$ - synthesis controller and the comparative simulation and reference results demonstrate the effectiveness of the presented active suspension system with  $\mu$ - synthesis controller.

**Keywords:** Quarter car active suspension system,  $H_{\infty}$  controller,  $\mu$  - synthesis controller, Robust controller

## INTRODUCTION

At present, the world's leading automotive companies and research institutions have invested considerable human and material resources to develop a cost-effective vehicle suspension system, in order to be widely used in the vehicle. The main aim of suspension system

is to isolate a vehicle body from road irregularities in order to maximize passenger ride comfort and retain continuous road wheel contact in order to provide road holding. Many studies have shown that the vibrations caused by irregular road surfaces have an energy-draining effect on drivers, affecting their physical and mental health [1]. Demands for better ride comfort and controllability of road vehicles like passenger cars has motivated to develop new type of suspension systems like active and semi active suspension systems. These electronically controlled suspension systems can potentially improve the ride comfort as well as the road handling of the vehicle. An active suspension system has the capability to adjust itself continuously to changing road conditions. By changing its character to respond to varying road conditions, active suspension offers superior handling, road feel, responsiveness and safety.

An active suspension system has the ability to continuously adjust to changing road conditions. By changing its character to respond to different road conditions, the active suspension offers superior handling, road feel, responsiveness and safety.

Active suspension systems dynamically respond to changes in the road profile because of their ability to supply energy that can be used to produce relative motion between the body and wheel. Typically, the active suspension systems include sensors to measure suspension variables such as body velocity,

suspension displacement, and wheel velocity and wheel and body acceleration. An active suspension is one in which the passive components are augmented by actuators that supply additional forces. These additional forces are determined by a feedback control law using data from sensors attached to the vehicle.

The existing active suspension system is inefficient if there are changes in parameter of the system or of actuator, then controlling the suspension system becomes a big problem.

Therefore  $H_{\infty}$  and  $\mu$  - synthesis control technique are used.  $H_{\infty}$  and  $\mu$  - synthesis control effectively suppresses the vehicle vibrations in the sensitive frequency range of the human body. The desired robust performance and robust stability are achieved in the closed loop system for a quarter vehicle model in the presence of structured uncertainties.

## MATHEMATICAL MODELS

### — Active Suspension System Mathematical Model

The mathematical model of the following subsection are only discussing the amount of force created by the active suspension. Active suspensions allow the designer to balance these objectives using hydraulic actuator which is driven by a motor between the chassis and wheel assembly. The actuator force  $f_s$  applied between the body and wheel assembly is represents the active component of the suspension system.

Most of the researchers choose to utility quarter vehicle dynamic shock model when they hubs on the vehicle body vertical vibration caused by the capacity of pavement roughness. Although quarter vehicle dynamic vibration configuration has not included the entire vehicle geometrical information, and it cannot

research the vehicle pitching angle shock and roll angle vibration.

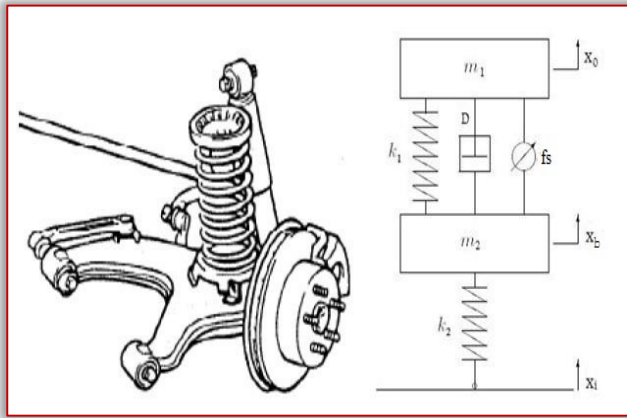


Figure 1: Quarter model of active suspension system with actuating force  $f_s$  between sprung and unsprung mass.

Figure 1 shows a vehicle quarter model of active suspension system. The mass  $m_1$  (in kilograms) represents the car chassis (body) and the mass  $m_2$  (in kilograms) represents the wheel assembly. The spring  $K_1$  and damper  $D$  represent the passive spring and shock absorber placed between the car body and the wheel assembly. The spring  $K_2$  models the compressibility of the pneumatic tire. The variables  $x_0$ ,  $x_b$  and  $x_i$  (all in meters) are the body travel, wheel travel, and road disturbance, respectively. The actuator force  $f_s$  (in kiloNewtons) applied between the body and wheel assembly is controlled by feedback and represents the active component of the suspension system.

From this model, we can analyze the vehicle suspension system dynamics as a linear system model and establish two degrees of freedom motion differential equations will be as follow:

$$m_1 \ddot{x}_0(t) + D[\dot{x}_0(t) - \dot{x}_2(t)] + k_1[x_0(t) - x_2(t)] = u$$

$$m_2 \ddot{x}_2(t) - D[\dot{x}_0(t) - \dot{x}_2(t)] + k_1[x_2(t) - x_0(t)] + k_2[x_2(t) - x_i(t)] = -u$$

We can set:

$$x_1 = x_2(t), x_2 = x_0(t), x_3 = \dot{x}_2(t), x_4 = \dot{x}_0(t)$$

The system state space equation can be express as:

$$\frac{dX}{dt} = AX + BU \quad (1)$$

In this equation, state variable matrixes are:

$$X = (x_1 \quad x_2 \quad x_3 \quad x_4)^T \quad (2)$$

Constant matrixes A and B are shown as below:

$$A = \begin{pmatrix} 0 & 0 & 1 & 0 \\ 0 & 0 & 0 & 1 \\ -\frac{k_1 + k_2}{m_2} & \frac{k_1}{m_2} & -\frac{D}{m_2} & \frac{D}{m_2} \\ \frac{k_1}{m_1} & -\frac{k_1}{m_1} & \frac{D}{m_1} & -\frac{D}{m_1} \end{pmatrix}$$

$$B = \begin{pmatrix} 0 & 0 \\ 0 & 0 \\ \frac{k_2}{m_2} & \frac{1}{m_2} \\ 0 & -\frac{1}{m_1} \end{pmatrix}$$

The system input variable matrix will be:

$$U = (x_1(t) \quad u)^T$$

The vehicle suspension system output matrix equation will be:

$$Y = CX + DU$$

In above equation, the output variable matrix Y will be:

$$Y = (k_2[x_1(t) - x_2(t)] \quad \ddot{x}_0(t) \quad x_0(t))$$

Y will also express as the following equation:

$$Y = (k_2[x_1(t) - x_2(t)] \quad \ddot{x}_0(t) \quad x_0(t))$$

Constant matrixes C and D will be shown as below:

$$C = \begin{pmatrix} -k_2 & 0 & 0 & 0 \\ \frac{k_1}{m_1} & -\frac{k_1}{m_1} & \frac{D}{m_1} & -\frac{D}{m_1} \\ 0 & 1 & 0 & 0 \end{pmatrix}$$

$$D = \begin{pmatrix} k_2 & 0 \\ 0 & -\frac{1}{m_1} \\ 0 & 0 \end{pmatrix}$$

### —Hydraulic Actuator System Mathematical Model

The hydraulic actuator consists of a variable stroke hydraulic pump and a fixed stroke hydraulic motor as shown in the below Figure 2. The device accepts a linear displacement (stroke length) input and delivers an angular displacement. The pump and motor attached with the wheel assembly and this arrangement attached with the car chassis through a metal chain. When a sudden road disturbance enters to the pump, high pressure oil will enter to the motor and the motor control the displacement between the wheel assembly and the car chassis.

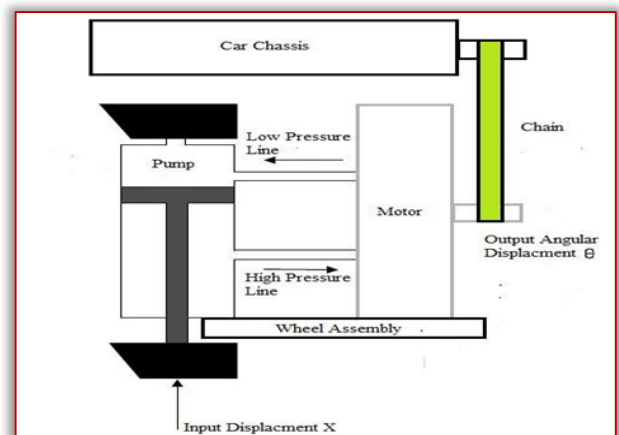


Figure 2: Hydraulic actuator block diagram

The hydraulic motor is controlled by the amount of oil delivered by the pump. By mechanically changing the pump stroke, the oil delivered by the pump is controlled. Like in a DC generator and dc motor, there is no essential difference between hydraulic pump and motor. In a pump the input is mechanical power and output is hydraulic power and in a motor, it is vice versa.

Let

$q_p$  Rate at which the oil flows from the pump

$q_m$  Oil flow rate through the motor

$q_i$  Leakage flow rate

$q_c$  Compressibility flow rate

$x$  Input stroke length

$\theta$  Output angular displacement of motor

$P$  Pressure drop across motor

The rate at which the oil flow from the pump is proportional to stroke speed, i.e.  $q_p \propto \frac{dx}{dt}$ .

Oil flow rate from-the pump,

$$q_p = K_p \frac{dx}{dt} \quad (3)$$

where

$K_p$  = Ratio of rate of oil flow to unit stroke angle.

The rate of oil flow through the motor is proportional to motor speed, i.e.  $q_m \propto \frac{d\theta}{dt}$ .

Oil flow rate through motor,

$$q_m = K_m \frac{d\theta}{dt} \quad (4)$$

where

$K_m$  = Motor displacement constant.

All the oil from the pump does not flow through the motor in the proper channels. Due to back pressure in the motor, a slices of the shape flow from the pump leaks back past the pistons of motor and pump. The back pressure is the importance that is built up by the hydraulic flow to overcome the hostility of free movement offered by load on motor shaft.

It is usually assumed that the leakage flow is proportional to motor pressure, i.e.  $q_i \propto P$ .

Leakage flow rate,

$$q_i = K_i P \quad (5)$$

where

$K_i$  = constant.

The back pressure built up by the motor not only causes leakage flow in the motor and pump but oil in the lines to compress. Volume compressibility flow is essentially proportional to pressure and therefore the tariff of flow is proportional to the rate of innovations

of pressure, i.e.  $q_c \propto \frac{dP}{dt}$

Compressibility flow rate,

$$q_c = K_c \frac{dP}{dt} \quad (6)$$

where

$K_c$  = Coefficient of compressibility.

The rate at which the oil flows from the pump is given by sum of oil flow tariff through the motor, leak flow rate and compressibility flow rate.

$$q_p = q_m + q_i + q_c$$

Substituting eqn. (3), (4), (5) and (6) from above equations, we get

$$K_p \frac{dx}{dt} = K_m \frac{d\theta}{dt} + K_i P + K_c \frac{dP}{dt} \quad (7)$$

The torque  $T_m$  developed by the motor is proportional to pressure drop and balances load torque.

Hydraulic motor torque,

$$T_m = K_t P \quad (8)$$

where

$K_t$  is motor torque constant.

If the load is assumed to consist of moment of inertia  $J$  and viscous friction with coefficient  $B$ ,

Then

Load Torque

$$T_l = J \frac{d^2\theta}{dt^2} + B \frac{d\theta}{dt} \quad (9)$$

$$\text{Hydraulic power input} = q_m P \quad (10)$$

Substituting eqn. (4) into eqn. (10), we get

$$\text{Hydraulic power input} = K_m \frac{d\theta}{dt} P \quad (11)$$

$$\text{Mechanical power output} = T_m \frac{d\theta}{dt} \quad (12)$$

Substituting eqn. (8) into eqn. (12), we get

$$\text{Mechanical power output} = K_t P \frac{d\theta}{dt} \quad (13)$$

If hydraulic motor losses are neglected or included as a part of load, then the hydraulic motor input is equal to mechanical power output of hydraulic motor.

$$K_m \frac{d\theta}{dt} P = K_t P \frac{d\theta}{dt} \quad (14)$$

From equation (14), it is clear that  $K_m = K_t$ .

Hence we can write

$$T_m = K_t P = K_m P$$

Since the motor torque equals load torque,  $T_m = T_l$

$$K_m P = J \frac{d^2\theta}{dt^2} + B \frac{d\theta}{dt} \quad (15)$$

$$P = \frac{J}{K_m} \frac{d^2\theta}{dt^2} + \frac{B}{K_m} \frac{d\theta}{dt} \quad (16)$$

Differentiating equation (16) w.r.t time, we get

$$\frac{dP}{dt} = \frac{J}{K_m} \frac{d^3\theta}{dt^3} + \frac{B}{K_m} \frac{d^2\theta}{dt^2} \quad (17)$$

Substituting for  $P$  and  $dP/dt$  to eqn.(7), we get,

$$K_p \frac{dx}{dt} = K_m \frac{d\theta}{dt} + K_i \left[ \frac{J}{K_m} \frac{d^2\theta}{dt^2} + \frac{B}{K_m} \frac{d\theta}{dt} \right] + K_c \left[ \frac{J}{K_m} \frac{d^3\theta}{dt^3} + \frac{B}{K_m} \frac{d^2\theta}{dt^2} \right] \quad (18)$$

Taking Laplace transform with zero initial conditions, we get,

$$\frac{\theta(s)}{X(s)} = \frac{K_p}{\left[ \frac{K_c J}{K_m} s^2 + \left[ \frac{K_i J + K_c B}{K_m} \right] s + \frac{K_m^2 + K_i B}{K_m} \right]} \quad (19)$$

In hydraulic systems, normally  $K_m \ll K_c$ , therefore, Put  $K_c = 0$  in above equation.

$$\frac{\theta(s)}{X(s)} = \frac{K_p}{\left[ \frac{K_i J}{K_m} s + \frac{K_m^2 + K_i B}{K_m} \right]} = \frac{K}{(\tau s + 1)} \quad (20)$$

where

$$K = \frac{K_p}{\frac{K_m^2 + K_i B}{K_m}} \text{ and } \tau = \frac{K_i J}{K_m^2 + K_i B}$$

$$K_p = 1$$

$$K_m = 4$$

where:  $K_i = -3$

$$B = 4$$

$$J = 16.67$$

The value of  $K$  and  $\tau$  is  $K=1$  and  $\tau = 1/50$

The transfer function of the hydraulic actuator is

$$\frac{\theta(s)}{X(s)} = \frac{1}{\frac{1}{50}s + 1}$$

## ROAD PROFILES

### — Bump Road Disturbance

Bump road disturbance is a basic input to research the suspension system. It simulated a very intense force for a very short time, such as a vehicle drive through a speed hump. This road disturbance has a maximum height of 5 cm as shown in Figure 3.

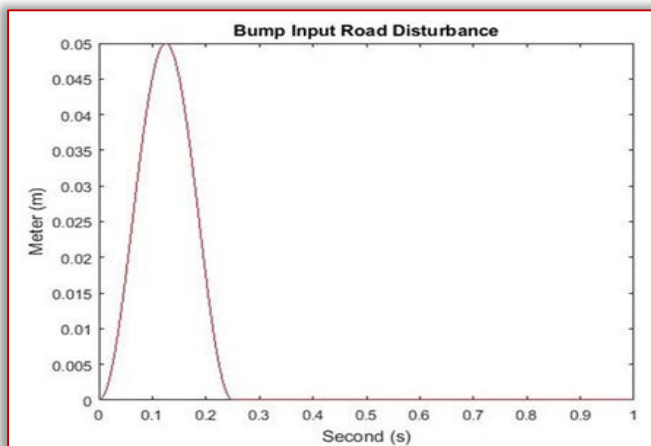


Figure 3: Bump road disturbance

### — Random Road Disturbance

Numerous researches shows that it is necessary to test a car to a random road disturbance to check the spring and damper respond quickly and correctly. The random road disturbance has a maximum height of 15 cm and minimum height of -15 cm as shown in Figure 4.

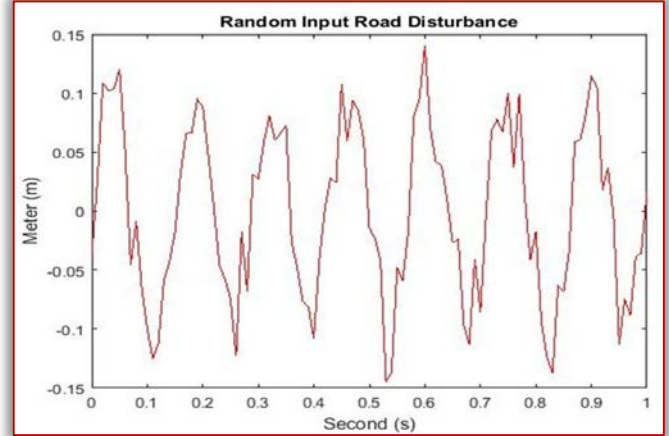


Figure 4: Random road disturbance

### — Sine Pavement Road Disturbance

Sine wave input signal can be used to simulate periodic pavement fluctuations. It can test the vehicle suspension system elastic resilience ability while the car experiences a periodic wave pavement. Sine input pavement test is made by every automotive industries before a new vehicle drives on road. The sine pavement road disturbance has a height of -10 cm to 10 cm as shown in Figure 5.

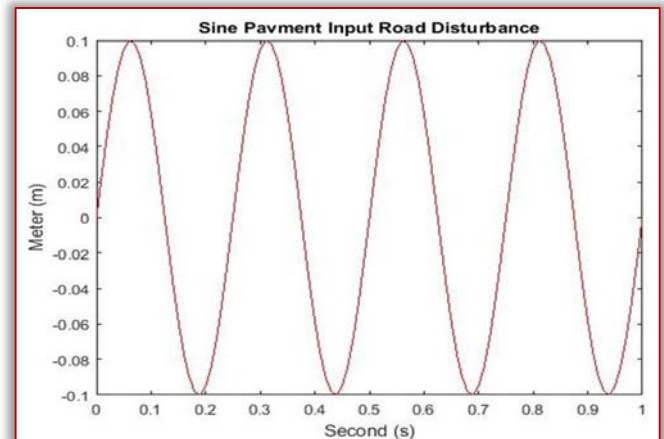


Figure 5: Sine pavement road disturbance

### — Harmonic Road Disturbance

Numerous researches show that when the vehicle speed is constant, harmonic road profile may be usually used in the simulation to verify the stability and capability of the designed control system, besides the system response status.

The harmonic road disturbance model is shown in Figure 6 with a maximum height of 5cm and a minimum height of -5cm.



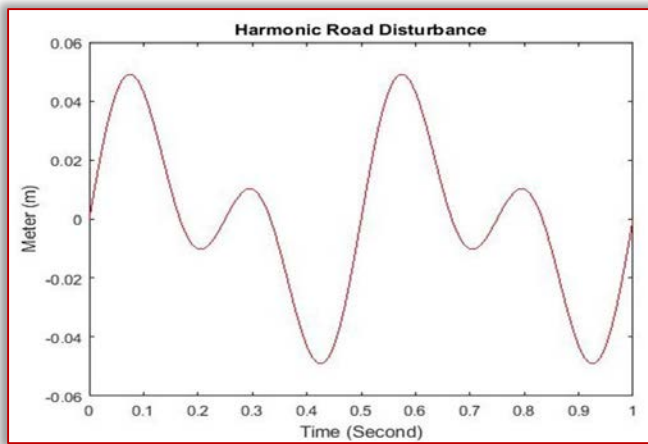


Figure 6: Harmonic road disturbance

### WEIGHTING FUNCTIONS

It is required that in the  $H^\infty$  framework to use weighting functions to reconciliation different performance objectives. The performance goal of a feedback system can be usually determined in terms of requirements on the sensitivity functions and/or complementary sensitivity functions or in terms of some other closed loop transfer functions. The odds of occupying weighted performance in multivariable system design is firstly, some part of a vector signal are usually more important than others, secondly, measuring each signal will not be in the same unit. For instance, some part of the output error signal may be measured in terms of length, and others may be measured in terms of voltage. Therefore, weighting functions play an essential rule to type these part comparable. The weighting functions are discussed below.

The weighting function  $W_{act}$  is used to limit the magnitude and frequency content of the active control force signal. Choosing

$$W_{act} = \frac{80}{11} \frac{s + 60}{s + 600}$$

$W_{x1}$  and  $W_{x1-x3}$  are used to keep the car deflection and the suspension deflection small over the desired range. The car body deflection  $W_{x1}$  is given as

$$W_{x1} = \frac{508.1}{s + 56.55}$$

The suspension deflection is used via weighting function  $W_{x1-x3}$ . The weighting function is given as

$$W_{x1-x3} = \frac{15}{0.2s + 1}$$

### THE PROPOSED CONTROLLER DESIGN

The design of active suspension system to provide passenger comfort and road handling is developed using  $H^\infty$  and  $\mu$ -synthesis controllers design. In the active suspension system, the proposed controllers design included the hydraulic actuator dynamics. In order to account for the difference between the actuator model and the actual actuator dynamics, a

first order model of the actuator dynamics as well as an uncertainty model have been used. The main aim of the controller design is to minimize suspension deflection, body acceleration and body travel of the system. Synthesis method is used to design the proposed controllers by achieving the performance objective via minimizing the weighted transfer function norm. The active suspension system with  $H^\infty$  and  $\mu$ -synthesis controllers with hydraulic motor actuator system interconnections block diagram is shown in Figure 7.

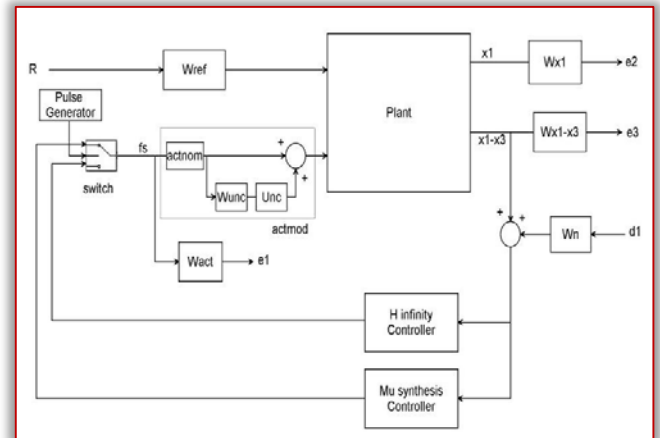


Figure 7: Active suspension system with  $H^\infty$  and  $\mu$ -synthesis controllers system interconnections block diagram

In Figure 7 plant represents the quarter car suspension model,  $H^\infty$  controller is a controller which is designed by  $H^\infty$  approach.  $e_1$ ,  $e_2$  and  $e_3$  are the first, second and third outputs after influencing weighting functions.

A  $\mu$ -synthesis controller is synthesized using D-K iteration. The D-K iteration method is an approximation to synthesis that attempts to synthesize the controller. There is two control input the road disturbance signal and the active control force. There are three measurement output signals, the suspension deflection, car body acceleration and car body travel. The pulse generator switches between the two systems in  $\mu$  seconds. In practice, the suspension deflection can be measured by acoustic or radar transmitter/receiver, while the velocity is typically obtained by integrating the acceleration which is measured using accelerometer.

There are two purposes for the weighted functions norm: for a given norm, there will be a direct comparison for different performance objectives and they are used for knowing the frequency information incorporated into the analysis. The output or feedback signal  $y$  is

$$y = ((x_1 - x_3) + d_1 \times W_n)$$

The controller's acts on the  $y$  signal to produce the active control force signal. The  $W_n$  block modelled

the sensor noise in the channel.  $W_n$  is given a sensor noise of 0.05m.

$$W_n = 0.05$$

$W_n$  is used to model the noise of the displacement sensor. The magnitude of the road disturbance is scaled using the weight  $W_{ref}$ . Let us assume the maximum road disturbance is 0.1m which means

$$W_{ref} = 0.1$$

## RESULT AND DISCUSSION

To ensure that our controller design achieves the desired objective, the closed loop active suspension system is simulated with the following parameter values as shown in Table 1.

Table 1: Parameters of quarter vehicle model

Model parameters	symbol	symbol Values
Vehicle body mass	m 1	300 Kg
Wheel assembly mass	m 2	40 Kg
Suspension stiffness	k 1	15,000 N/m
Tyre stiffness	k 2	150,000 N/m
Suspension damping	D	1000 N-s/m

### —Active Suspension System Control Targets Simulation Output Specifications

Each active suspension system control targets (body travel, body acceleration and suspension deflection) has its own output specifications while the vehicle in motion.

The body travel output should be the minimum vertical amplitude because the passenger must not feel the road disturbance while the vehicle in motion. In an ideal suspension system, the body travel vertical amplitude is zero.

The body acceleration output should be the minimum vertical acceleration because the passenger must not feel the sudden vertical acceleration while the vehicle hits the road disturbance. In an ideal suspension system, the vertical velocity is constant.

The suspension deflection output should be the same as the road disturbance input because if it is above or below the road disturbance input, it will affect the body travel output.

### —Time Domain Comparison of the Active Suspension System with $H_\infty$ and $\mu$ - synthesis Controllers

In this subsection, we simulate the active suspension system with  $H_\infty$  controller and active suspension system with  $\mu$  - synthesis controller for suspension deflection, body acceleration and body travel using bump, random, sine pavement and harmonic road disturbances.

#### » Simulation of a Bump Road Disturbance

The simulation for a bump input road disturbance is shown below. In this simulation, we simulate active

suspension system with  $H_\infty$  controller and active suspension system with  $\mu$  - synthesis controller for suspension deflection, body acceleration and body travel.

The body travel, body acceleration and suspension deflection simulation output is shown in Figure 8, Figure 9 and Figure 10 respectively for a bump road disturbance.

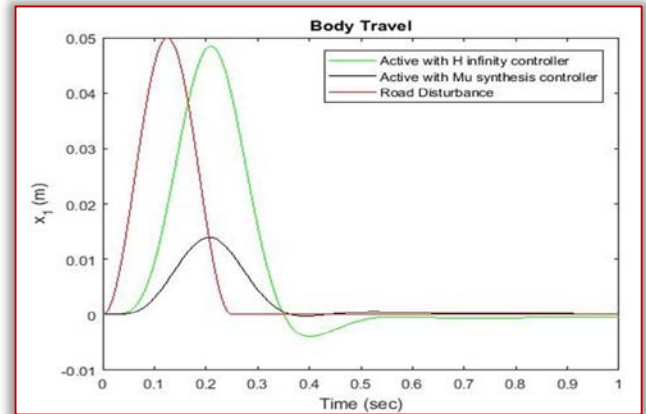


Figure 8: Body travel for bump road disturbance

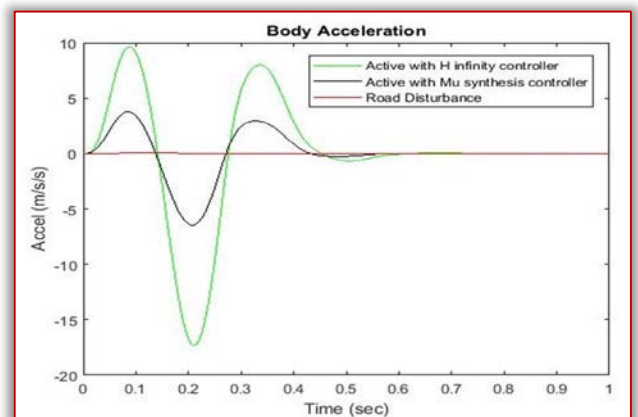


Figure 9: Body acceleration for bump road disturbance

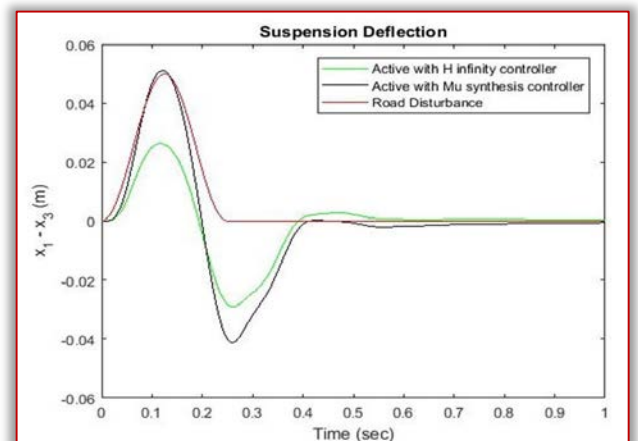


Figure 10: Suspension deflection for bump road disturbance

#### » Simulation of a Random Road Disturbance

The simulation for a random input road disturbance is shown below. In this simulation, we simulate active suspension system with  $H_\infty$  controller and active

suspension system with  $\mu$  - synthesis controller for suspension deflection, body acceleration and body travel.

The body travel, body acceleration and suspension deflection simulation output is shown in Figure 11, Figure 12 and Figure 13 respectively for a random road disturbance.

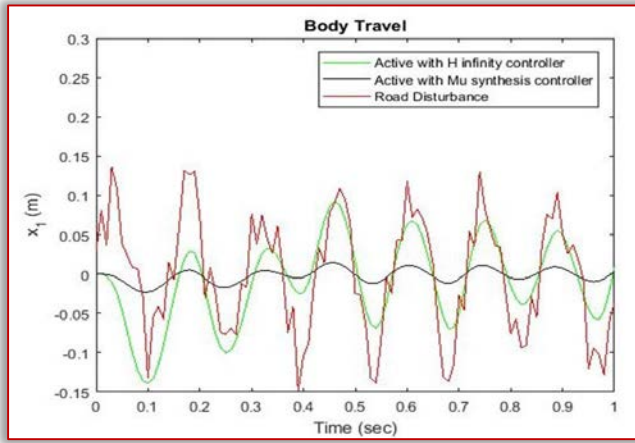


Figure 11: Body travel for random road disturbance

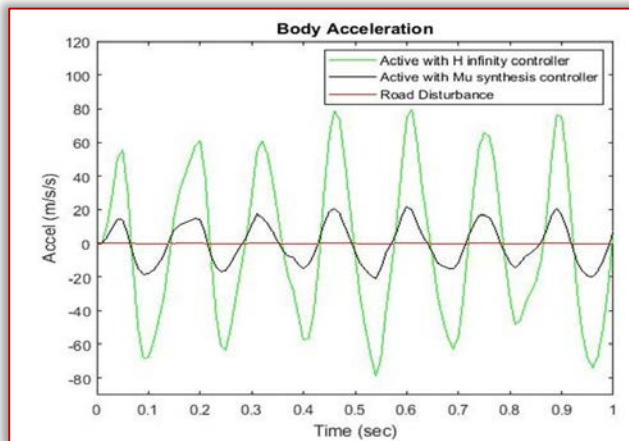


Figure 12: Body acceleration for random road disturbance

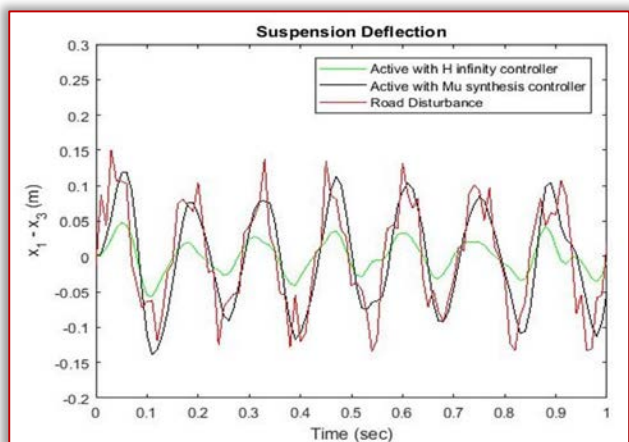


Figure 13: Suspension deflection for random road disturbance

### » Simulation of a Sine Pavement Input Road Disturbance

The simulation for a sine pavement input road disturbance is shown below. In this simulation, we simulate active suspension system with  $H^\infty$  controller and active suspension system with  $\mu$  - synthesis controller for suspension deflection, body acceleration and body travel.

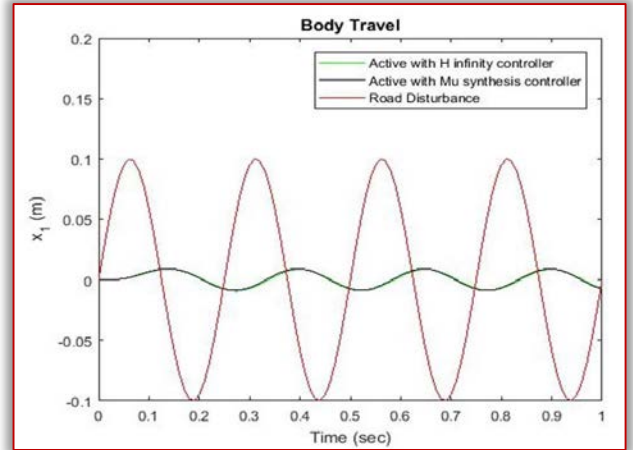


Figure 14: Body travel for sine input pavement road disturbance

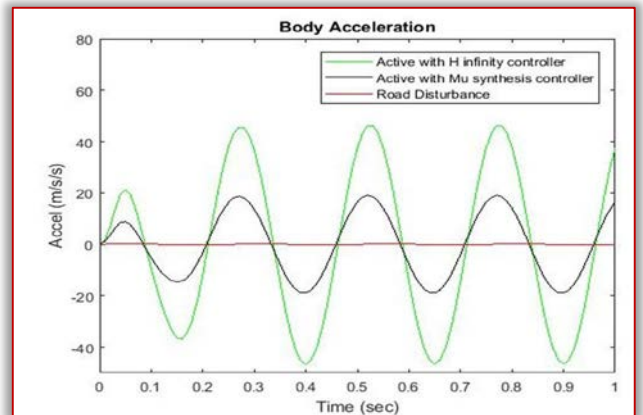


Figure 15: Body acceleration for sine input pavement road disturbance

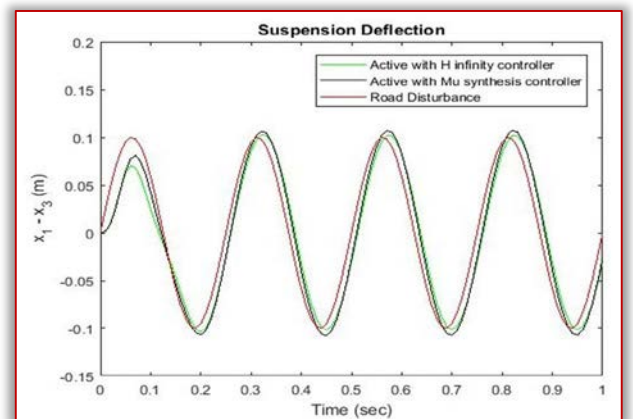


Figure 16: Suspension deflection for sine input pavement road disturbance



The body travel, body acceleration and suspension deflection simulation output is shown in Figure 14, Figure 15 and Figure 16 respectively for a sine pavement road disturbance.

» **Simulation of a Harmonic Road Disturbance**

The simulation for a harmonic input road disturbance is shown below. In this simulation, we simulate active suspension system with  $H^\infty$  controller and active suspension system with  $\mu$ -synthesis controller for suspension deflection, body acceleration and body travel.

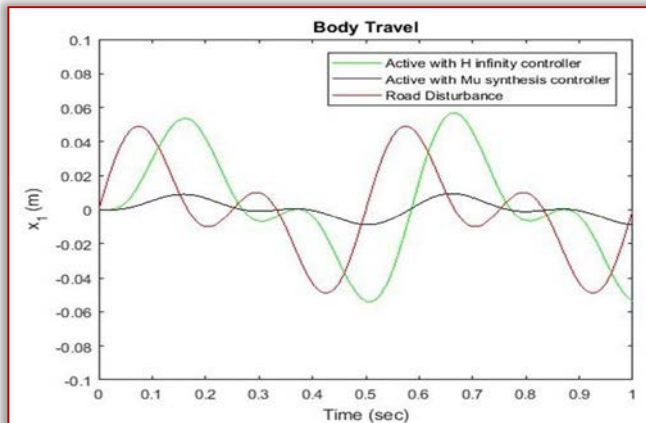


Figure 17: Body travel for harmonic road disturbance

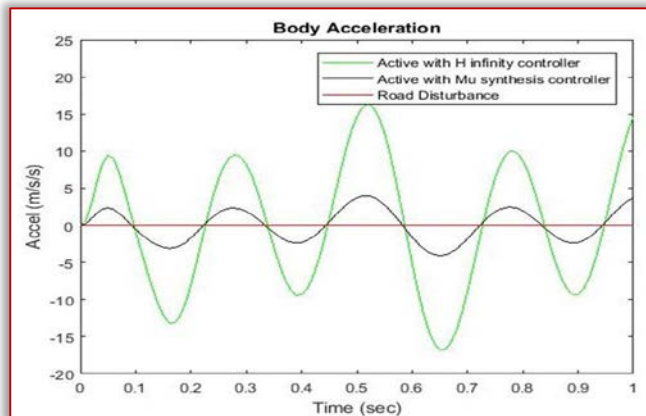


Figure 18: Body acceleration for harmonic road disturbance

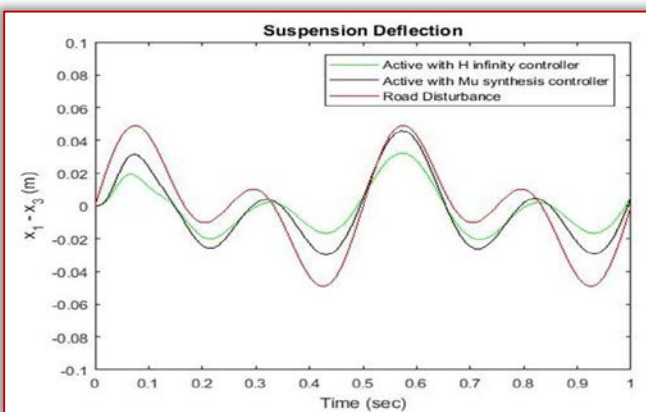


Figure 19: Suspension deflection for harmonic road disturbance

The body travel, body acceleration and suspension deflection simulation output is shown in Figure 17, Figure 18 and Figure 19 respectively for a harmonic road disturbance.

— **Frequency Domain Comparison of the Active Suspension System with  $H^\infty$  and  $\mu$ -synthesis Controllers**

The frequency domain analysis of the active suspension system with  $H^\infty$  controller and active suspension system with  $\mu$ -synthesis controller to body travel, body acceleration and suspension deflection is presented below.

» **Body Travel**

The bode plot comparison of the active suspension system with  $H^\infty$  controller and active suspension system with  $\mu$ -synthesis controller for body travel is shown in Figure 20 below.

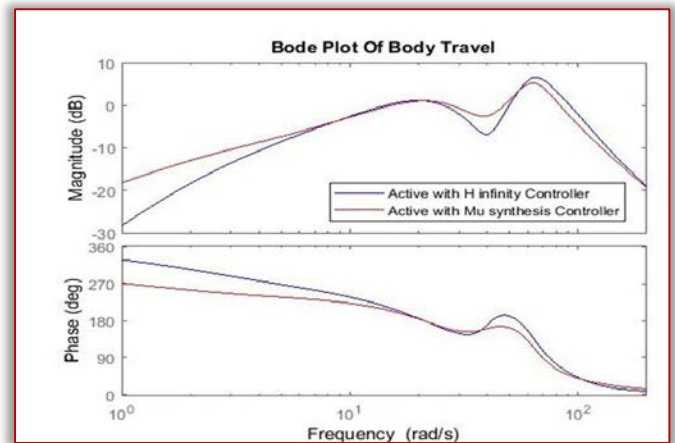


Figure 20: Bode plot of body travel

— **Body Acceleration**

The bode plot comparison of the active suspension system with  $H^\infty$  controller and active suspension system with  $\mu$ -synthesis controller for body acceleration is shown in Figure 21 below.

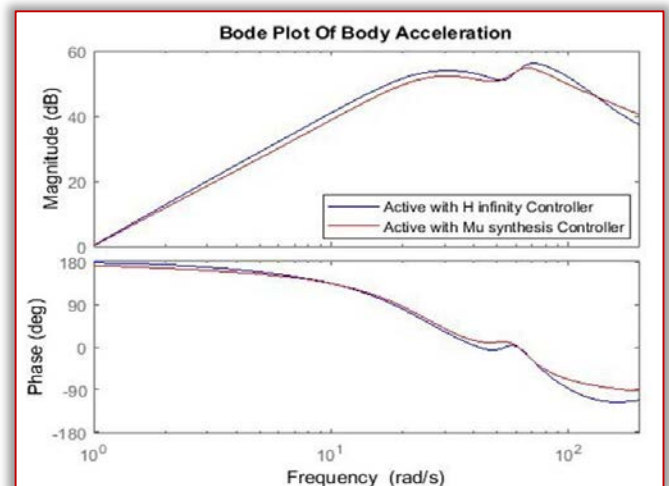


Figure 21: Bode plot of body acceleration



» **Suspension Deflection**

The bode plot of the active suspension system with  $H^\infty$  controller and active suspension system with  $\mu$  - synthesis controller for suspension deflection is shown in Figure 22 bellow.

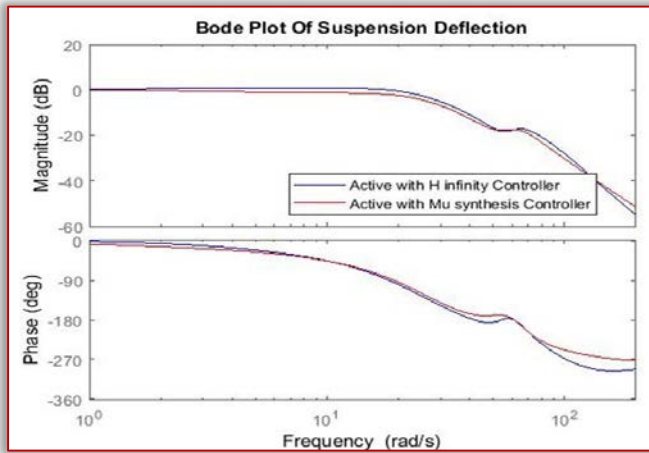


Figure 22: Bode plot of Suspension deflection

— **Frequency Domain Comparison Result of Active Suspension System with  $H^\infty$  and  $\mu$  - synthesis Controllers**

While in motion, human body is more prone to the possessions of shock in the frequency cord of 10–20 Hz. Figures 20, Figure 21 and Figure 22 shows the frequency feedback plot of suspension deflection, body acceleration and body travel of robust H-infinity and robust Mu-synthesis technique. From the result, it is evident that there exist two natural frequency which can be classified as lower frequency and higher frequency.

At higher frequency, the active controller with mu-synthesis controller shows a good response, whereas, at lower frequency, both the active controller with H infinity and mu-synthesis controllers is more effective is suppressing the vibration.

Comparing all the results, it is clear that at higher frequency, the active controller with mu-synthesis controller shows a good response and both H infinity and mu-synthesis controller has best performance in controlling the shock at low frequency region.

— **Numerical Values of the Simulation Outputs**

The numerical values of the simulation output for the control targets body travel, body acceleration and suspension deflection for the four road disturbances is shown in Table 2, Table 3 and Table 4 bellow.

Table 2: Numerical values of the body travel simulation output

No	Systems	Bump	Random	Sine	Harmonic
1	Road Profile	0.05m	0.15m	0.1m	0.05m
2	$H^\infty$	0.049m	0.09m	0.01m	0.055m
3	$\mu$ - synthesis	0.013m	0.01m	0.01m	0.011m

Table 2 shows us the active suspension system with  $\mu$  - synthesis controller have the minimum body travel amplitude in the random road disturbance and the active suspension system with  $\mu$  - synthesis controller shows the best performance in the random road profile.

Table 3: Numerical values of the body acceleration simulation output

No	Systems	Bump	Random	Sine	Harmonic
1	Road Profile	1 m/s <sup>2</sup>	5 m/s <sup>2</sup>	2 m/s <sup>2</sup>	1 m/s <sup>2</sup>
2	$H^\infty$	10 m/s <sup>2</sup>	80 m/s <sup>2</sup>	45 m/s <sup>2</sup>	16 m/s <sup>2</sup>
3	$\mu$ - synthesis	4 m/s <sup>2</sup>	20 m/s <sup>2</sup>	18 m/s <sup>2</sup>	3 m/s <sup>2</sup>
8	$H^\infty$ Loop Shaping	5.5 m/s <sup>2</sup>	40 m/s <sup>2</sup>	30 m/s <sup>2</sup>	15 m/s <sup>2</sup>

Table 3 shows us the active suspension system with  $\mu$  - synthesis controller have the minimum body acceleration amplitude in the harmonic road disturbance and the active suspension system with  $\mu$  - synthesis controller shows the best performance in the harmonic road profile.

Table 4: Numerical values of the suspension deflection simulation output

No	Systems	Bump	Random	Sine	Harmonic
1	Road Profile	0.05m	0.14m	0.1m	0.05m
2	$H^\infty$	0.022m	0.05m	0.1m	0.03m
3	$\mu$ - synthesis	0.05m	0.14m	0.1m	0.05m

Table 4 shows us the active suspension system with  $\mu$  - synthesis controller have the suspension deflection amplitude the same as the road disturbance input in all the four road disturbances and the active suspension system with  $\mu$  - synthesis controller shows the best performance in all the four road disturbances.

**CONCLUSIONS**

In this paper,  $H^\infty$  controller and  $\mu$  - synthesis controllers are successfully designed using MATLAB/Script for quarter car active suspension system.

The design of a MATLAB script that represents the active suspension system with  $H^\infty$  controller and  $\mu$  - synthesis controller have been done and tasted with bump, sine input pavement, random and harmonic road disturbances for body travel, body acceleration and suspension deflection.

The comparison of the time and frequency domain of the active suspension system with  $H^\infty$  controller and  $\mu$  - synthesis controller for the body travel, body acceleration and suspension deflection have been analyzed.

In the time domain analysis, we have tested the two systems with bump, sine input pavement, harmonic and random road disturbances and the comparative simulation and reference results prove the effectiveness of the presented active suspension with  $\mu$  - synthesis controller.

In the frequency domain analysis, the results shows that at higher frequency, the active suspension system with  $\mu$  - synthesis controller shows a good response and at low frequency region, both the active suspension system with  $H_{\infty}$  controller and the active suspension system with  $\mu$  - synthesis controller has best performance in controlling the vibration.

Finally the comparative simulation and reference results prove the effectiveness of the presented active suspension with  $\mu$  - synthesis controller and it achieves the passenger comfort and road handling criteria that needed to make the active suspension system is the best suspension system.

#### Acknowledgment

First and foremost, I would like to express my deepest thanks and gratitude to Dr. Parashante and Mr. Tesfabirhan for their invaluable advices, encouragement, continuous guidance and caring support during my journal preparation.

Last but not least, I am always indebted to my brother, Taha Jibril, my sister, Nejat Jibril and my family members for their endless support and love throughout these years. They gave me additional motivation and determination during my journal preparation.

#### References

- [1] Gang Wang, Zhijin Zhou, Design and Implementation of  $H_{\infty}$  Miscellaneous Information Feedback Control for Vehicle Suspension System, Shock and Vibration Volume, ID 3736402, 15 pages, 2019.
- [2] Peter Benner, Tim Mitchell, Faster and More Accurate Computation of the  $H_{\infty}$  Norm via Optimization, Society for Industrial and Applied Mathematics, Vol. 40, No. 5, pp. A3609-A3635, 2018.
- [3] J. Marzbanrad, N. Zahabi,  $H_{\infty}$  Active Control of a Vehicle Suspension System Exited by Harmonic and Random Roads, Journal of Mechanics and Mechanical Engineering, Vol. 21, No. 1, pp 171-180, 2017.
- [4] Kruczek Ales, Stribrsky Antonin, Automotive active suspension – case study on H-infinity control, Recent Researches in Automatic Control, 2017.
- [5] Wang Chun Yan, Deng K, Robust Control for Active Suspension System Under Steering Condition, Science China Press, Springer-Verlag Berlin, Heidelberg, 2017.
- [6] Katerina Hyniova, One-Quarter-Car Active Suspension Model Verification, ITM Web of Conferences 9, 03003, 2017.
- [7] Abdoljalil Addeha, Abolfazl Ebrahimi, Optimal Design of Robust Controller for Active Car Suspension System Using Bee's Algorithm, Journal of Computational Research Progress in Applied Science & Engineering, ©PEARL publication, 2016.
- [8] Nouby M Ghazaly, Abdel-Nasser Sharkawy,  $H_{\infty}$  Control of Active Suspension System for a Quarter

Car Model, International Journal of Vehicle Structures and Systems, 2016.

- [9] Ales Kruczek, Antonin Stribrsky,  $H_{\infty}$  Control of Automotive Active Suspension with Linear Motor, M&MT project no. LN00B073 - Josef Bodek's Research Center of Combustion Engines and Automobiles, 2016.
- [10] Gaurav Kumar Sinha, Vibration Control of Car Suspension System Using Different Controllers, International Journal of Advance Reseach in Science and Engineering, Vol. No.6, Issue No.4, April, 2016.
- [11] Katerina Hyniova, On Testing of Vehicle Active Suspension Robust Control on An One-Quarter-Car Test Stand, International Journal of Mechanical Engineering, Volume 1, 2016.
- [12] Narinder Singh, Himanshu Chhabra, Robust Control of Vehicle Active Suspension System, International Journal of Control and Automation Vol. 9, No. 4 (2016), pp. 149-160.
- [13] Panshuo Li, James Lam, Kie Chung Cheung, Experimental Investigation of Active Disturbance Rejection Control for Vehicle Suspension Design, International Journal of Theoretical and Applied Mechanics, Volume 1, 2016.



ACTA TECHNICA CORVINIENSIS – Bulletin of Engineering  
ISSN: 2067-3809

copyright © University POLITEHNICA Timisoara,  
Faculty of Engineering Hunedoara,  
5, Revolutiei, 331128, Hunedoara, ROMANIA  
<http://acta.fih.upt.ro>